Flipped halfwave: improved modeling of spontaneous breathing effort

Joey Reinders [*,**] **Lars van de Kamp** [*,**] **Bram Hunnekens** [*]
Tom Oomen [**] **Nathan van de Wouw** [**,***]

[*] *DEMCON Advanced Mechatronics, Best, The Netherlands.*
[**] *Department of Mechanical Engineering, Eindhoven University of Technology, Eindhoven, The Netherlands.*
[***] *Department of Civil, Environmental and Geo- Engineering, University of Minnesota, Minneapolis, MN 55455 USA.*

Abstract: Spontaneous breathing effort of a mechanically ventilated patient can seriously deteriorate the treatment outcome if it is not taken into account when choosing the appropriate settings. This paper presents an improved spontaneous breathing effort model that can be used to develop improved mechanical ventilation algorithms. Through an indicative experimental study it is shown that this model accurately describes the spontaneous breathing effort of a healthy human test subject. In comparison to the commonly used sinusoidal halfwave effort model it is shown that the proposed model improved fitting quality by a factor two.

Keywords: Mechanical ventilation, Respiratory systems, Modeling, Breathing effort

1. INTRODUCTION

Mechanical ventilation is a life-saving therapy used in Intensive Care Units (ICUs) to assist patients who need support to breathe sufficiently. The main goals of mechanical ventilation are to ensure oxygenation and carbon dioxide elimination (Warner and Patel, 2013). Especially during the flu season or a world-wide pandemic such as the COVID-19 pandemic (Wells et al., 2020), mechanical ventilation is a common treatment for many patients around the world.

Mechanical ventilators are complex mechatronic systems with a wide variety of ventilation modes and complex algorithms to track the patient's clinical condition and synchronize a ventilator with the patient's effort. For the development of these algorithms, simulations and experiments in a controlled lab environment, with a lung emulator, are key. Such simulations and experiments are used for the development and validation of controllers, see Reinders et al. (2021); Borrello (2001); Hunnekens et al. (2020), for the development of algorithms to estimate the patient's spontaneous breathing effort, see Vicario et al. (2015), and for the development and analysis of algorithms to detect Patient-Ventilator Asynchrony (PVA), see Van Diepen et al. (2021). Development of such algorithms helps to assist the medical staff during the treatment of patients and even improve the treatment. According to Mauri et al. (2017); Yoshida et al. (2012), spontaneous breathing effort of the patient, if not taken into account, can seriously damage the lungs. Furthermore, excessive PVA can result in prolonged ICU stay and is even associated with increased mortality, see Epstein (2011); Thille et al. (2006); Blanch et al. (2015). Therefore, development of improved control and monitoring algorithms is potentially life-saving.

The improvement of these ongoing innovations on real patients hinges on the accuracy of the patient effort model. Therefore, a variety of lung mechanics and effort models are presented in literature. A wide variety of lung mechanics models is described in Bates (2009), varying from linear one-compartmental lung models to complex nonlinear multi-compartmental models. Also in Van Diepen et al. (2021), a wide variety of patient models is used to model patients with different clinical conditions. Besides models of the lung mechanics, models of the patient's spontaneous breathing effort are used. These models are essential to accurately model and analyze one of the big challenges in ventilation, namely, PVA. In Chiew et al. (2015); Van Drunen et al. (2014); Kim et al. (2017), the patient's spontaneous breathing effort is modeled as a time-varying elasticity of the lungs. Another, more common and intuitive, method is to model the breathing effort as a disturbance to the lung pressure induced by the downward motion of the diaphragm. This method is used in for example Scheel et al. (2017); Vicario et al. (2015); Navajas et al. (2000). However, as is pointed out in Olivieri et al. (2011); Fresnel et al. (2014), there is no consensus yet on the optimal shape for this disturbance. The most commonly used effort model is the sinusoidal halfwave (Fresnel et al., 2014).

Although a variety of breathing effort models have been proposed, the resulting flow patterns typically do not match the patterns seen in breathing of a human. Therefore, in this paper, a simple and intuitive breathing effort model is presented, to accurately model a human's breathing behavior. The presented model is verified by conducting an experiment with a healthy human test subject in a lab environment. By using a simple lung mechanics model and estimation approach, the breathing effort of the test subject is estimated. Then, in a simulation environment the proposed model and the sinusoidal halfwave are compared to the experimental results.

The main contribution of this paper is the presentation of an intuitive, simple breathing effort model that can be used for modeling patient-ventilator interaction, development of ventilation algorithms, and understanding of a patient's breathing

behavior. The presented model is validated and compared to the widely used sinusoidal halfwave through experiments and simulations.

The outline of the remainder of this paper is as follows. In Section 2, the considered lung mechanics model is presented. Thereafter, in Section 3, the new effort model and the commonly used sinusoidal halfwave are presented and compared. Thereafter, in Section 4, experiments are conducted to obtain realistic effort estimates. These experimental results are used to compare the proposed model and the sinusoidal halfwave to the real effort estimates. Finally, in Section 5, the main conclusions of this paper are summarized.

2. THE LUNG MECHANICS MODELS

The lung mechanics model considered in this paper is a linear one-compartmental lung model, which is extensively described in (Bates, 2009, pp. 37–60). In Fig. 1, a schematic representation of a simplified respiratory system with the relevant parameters and signals is depicted. The patient model without breathing effort is modeled by an airway model and a lung model. The airway model describes the relation between the pressure drop over the airway and the patient flow Q_{pat}. The lung model gives the relation between patient flow Q_{pat} and the pressure inside the lungs, i.e., lung pressure p_{lung}.

The airway is modeled using a linear resistance R_{lung}. This linear resistance gives the relation between the airway pressure, the lung pressure, and the patient flow:

$$Q_{pat}(t) = \frac{p_{aw}(t) - p_{lung}(t)}{R_{lung}}, \qquad (1)$$

where p_{aw} is the airway pressure, the pressure near the patients mouth, and p_{lung} is the lung pressure, the pressure inside the lungs. Note that p_{lung} is not measured in practice.

The lung model describes the relation between the patient volume V_{pat}, i.e., the volume inside the lungs, and the lung pressure p_{lung}. This relation is described by a linear lung compliance C_{lung}. The pressure inside the lungs is expressed as

$$p_{lung}(t) = \frac{1}{C_{lung}} \underbrace{\int_{t_0}^{t} Q_{pat}(\tau)d\tau}_{V_{pat}(t)} + p_{lung}(t_0), \qquad (2)$$

where integration of the flow over time gives the patient volume V_{pat} and $p_{lung}(t_0)$ is the initial lung pressure at time t_0.

Contraction and relaxation of the respiratory muscles induce the breathing effort p_{mus}. This breathing effort is modeled as an additive disturbance to the lung pressure in (2). More details on the breathing effort are presented in Section 3. Including the breathing effort p_{mus} in (2) gives the following equation for the lung pressure p_{lung}:

$$p_{lung}(t) = \frac{1}{C_{lung}} \underbrace{\int_{t_0}^{t} Q_{pat}(\tau)d\tau}_{V_{pat}(t)} + p_{lung}(t_0) + p_{mus}(t). \qquad (3)$$

Combining (1) and (3), results in the following expression for the patient flow, which is used in the experiments to obtain an estimate of p_{mus}:
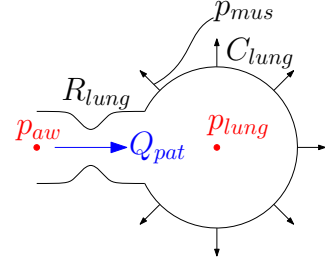

Fig. 1. Schematic representation of the patient's respiratory system, with the relevant patient parameters and signals. The signals p_{aw} and Q_{pat} are typically measured during mechanical ventilation.

$$Q_{pat}(t) = \frac{1}{R_{lung}} \left(p_{aw}(t) - \frac{1}{C_{lung}} V_{pat}(t) - R_{lung}Q_{pat}(t) \right.$$
$$\left. - p_{lung}(t_0) - p_{mus}(t) \right). \qquad (4)$$

Eventually, differentiation of (3) and using (1) as an output gives the following state-space model:

$$\dot{p}_{lung} = -\frac{1}{C_{lung}R_{lung}} p_{lung} + \frac{1}{C_{lung}R_{lung}} p_{aw} + \dot{p}_{mus},$$
$$Q_{pat} = -\frac{p_{lung}}{R_{lung}} + \frac{p_{aw}}{R_{lung}} \qquad (5)$$

with input p_{aw}, output Q_{pat}, state p_{lung}, and disturbance $\dot{p}_{mus}$, which is the time-derivative of the breathing effort p_{mus}. This state-space model is used to compare the different effort models to the experimental results. Next, these effort models are described.

3. BREATHING EFFORT MODELS

Breathing effort enables a person, i.e., healthy or patient, to inhale and exhale air by themselves. The breathing effort p_{mus} is modeled as a disturbance to the lung pressure p_{lung}. Using a simplified explanation of breathing, the relation between this disturbance and actual breathing is described. The breathing effort is mainly induced by a contraction of the diaphragm, which results in a downward motion of the diaphragm. This downward motion results in an increase in the pleural cavity, i.e., the volume around the lungs. This increase in volume results in a decreasing pressure inside the lungs and therewith air will flow into the lungs, in other words, an inspiration can be modeled by a decreasing value of p_{mus} in (3). Then, after some time, the diaphragm will relax and therewith the pleural cavity will decrease in volume again. This results in an increasing lung pressure, resulting in an air flow out of the patient's lungs. This expiration is modeled by an increase of p_{mus} towards zero, we assume passive expiration, i.e., $p_{mus}(t) \leq 0 \ \forall t \geq 0$.

In the remainder of this section, the newly proposed flipped halfwave breathing effort model is presented. Furthermore, for comparison, the commonly used sinusoidal halfwave effort model and simulation results of both models are presented.

3.1 Flipped halfwave effort model

Based on visual inspection of the resulting patient flow during simulations and experiments with the commonly used sinusoidal halfwave, it is concluded that the expiration phase of the sinusoidal halfwave contains some unnatural phenomenon, this is shown in Section 3.3. Therefore, the flipped halfwave is
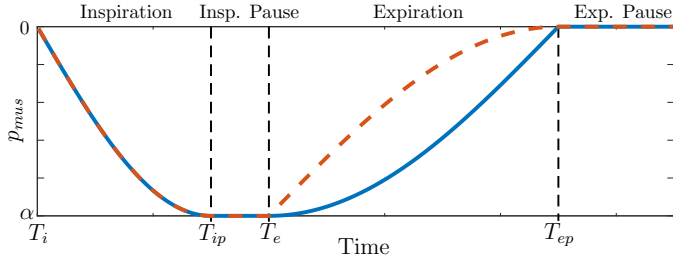
Fig. 2. Examples of both breathing effort models, i.e., the flipped halfwave (6) (- - -) and the sinusoidal halfwave (7) (——). The figure indicates all parameters that describe the different effort models, i.e., α, T_i, T_{ip}, T_e, and T_{ep}. Furthermore, it shows that the models are significantly different during the expiration phase.

proposed as an alternative effort model. The model is similar to the sinusoidal halfwave, only during expiration its shape is different from the sinusoidal halfwave. The *flipped halfwave*, can be described mathematically as follows:

$$p_{mus}(t) = \begin{cases} \alpha \sin\left(\dfrac{(t-T_i)\pi}{2(T_i - T_{ip})}\right), & T_i < t < T_{ip} \\ \alpha, & T_{ip} \leq t < T_e \\ \alpha \sin\left(\dfrac{(t-T_e)\pi}{2(T_{ep}-T_e)} + \pi\right) + \alpha, & T_e \leq t < T_{ep} \\ 0, & T_{ep} \leq t \end{cases} \quad (6)$$

In this model α represents the breath depth, which typically has a negative value, and the timing parameters T_i, T_{ip}, T_e, and T_{ep} are visualized in Fig. 2. The start time of the patient's inspiration is defined as T_i. Thereafter, an inspiratory pause starts at T_{ip}. The patient's expiration starts at T_e. Finally, at T_{ep} an expiratory pause is started. After this expiratory pause, a new breath can be initiated.

3.2 Sinusoidal halfwave effort model

For comparison with the sinusoidal halfwave, the sinusoidal halfwave is presented in this section. The *sinusoidal halfwave*, can be described mathematically as follows:

$$p_{mus}(t) = \begin{cases} \alpha \sin\left(\dfrac{(t-T_i)\pi}{2(T_i - T_{ip})}\right), & T_i \leq t < T_{ip} \\ \alpha, & T_{ip} \leq t < T_e \\ \alpha \sin\left(\dfrac{(t-T_e)\pi}{2(T_{ep}-T_e)} + \dfrac{\pi}{2}\right), & T_e \leq t < T_{ep} \\ 0, & T_{ep} \leq t \end{cases} \quad (7)$$

This model is similar to the presented flipped halfwave, only for $T_e \leq t < T_{ep}$ the sine function is flipped. Again α represents the breath depth, and the timing parameters T_i, T_{ip}, T_e, and T_{ep} are visualized in Fig. 2. Next, both effort models are compared through simulations.

3.3 Simulation based comparison of both effort models

Using (5) and the breathing effort models in (6) and (7), a simulation study is done to compare both effort models in terms of resulting patient flow Q_{pat}. For this simulation all pressures are defined relative to the ambient pressure, i.e., $p_{amb} = 0$ mbar. Furthermore, it is assumed that the patient is breathing in ambient air, i.e., $p_{aw}(t) = 0$ mbar $\forall t \geq 0$ and $p_{lung}(t_0) = 0$ mbar. The results are depicted in Fig. 3, with the lung parameters
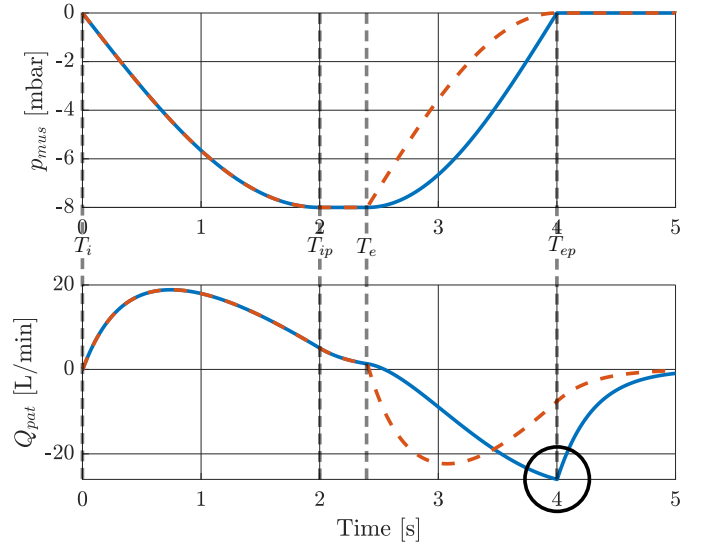

Fig. 3. Simulation results of both breathing effort models in the top figure and the resulting patient flow in the bottom figure. The figures show cases for the flipped halfwave (6) (- - -) and the sinusoidal halfwave (7) (——). From the figures it is concluded that during the expiration the proposed flipped halfwave shows a more natural expiration flow curve.

$R_{lung} = 5 \times 10^{-3}$ mbar s/mL and $C_{lung} = 60$ mL/mbar, breath depth $\alpha = -8$ mbar, and the breath timings are indicated in the figure.

The figure clearly shows that the inspiration phases for both models are exactly the same. However, the expiration phases are significantly different. In the simulation with the sinusoidal halfwave, the patient flow slowly decreases at the expiration start T_e. Then, at the end of the expiration, inside the circle at T_{ep}, the flow sharply changes direction which is an unnatural phenomenon compared to a humans normal breathing, as is experimentally shown in Section 4. In contrast, the flipped halfwave shows a fast decreasing patient flow at the start of the expiration, at T_e. Thereafter, it slowly converges towards zero without this sharp bend, which is intuitively more natural. Concluding, the resulting flow of the flipped halfwave is symmetrical and more smooth, which is intuitively more realistic. In Section 4, both models are compared to breathing of a human test subject in an experimental setting to validate this intuitive preference for the flipped halfwave breathing effort model.

4. EXPERIMENTAL VALIDATION OF THE BREATHING EFFORT MODEL

In this section, an experimental study is conducted to compare the effort models in (6) and (7) to healthy human test subjects. Although measurements on several subjects have been conducted, only one is shown in detail for simplicity; the overall conclusions are similar for all subjects. The goal of these experiments is to validate that the flipped halfwave represents the actual breathing effort accurately. The experimental setup and approach are described in Section 4.1. Thereafter, in Section 4.2, the experimental results are presented and the effort models presented in Section 3 are compared to the experimental results.

4.1 Experimental setup and approach

To obtain the experimental results, a test subject is breathing through a flow and pressure sensor with a bacterial filter. Using the sensors, the patient flow Q_{pat}, airway pressure p_{aw}, and patient volume V_{pat} are measured. Then, using the patient flow Q_{pat}, airway pressure p_{aw}, patient volume V_{pat}, the lung mechanics model in (4), and an educated guess for C_{lung} and R_{lung}, an estimate for p_{mus} is obtained. Using this estimate of p_{mus}, the parameters for the models in (6) and (7) are estimated. Finally, using the simulation model in (5) and the estimated effort models, a simulation study is conducted to compute the resulting patient flow Q_{pat} of both models. This flow is compared to the actual measured flow.

4.2 Experimental results

The measured data of the test subject is shown in the top and middle plot of Fig. 4. Using the measured patient flow, airway pressure, and (4), the true breathing effort p_{mus} is estimated. To compute the breathing effort, estimates of the airway resistance, $R_{lung} = 10 \times 10^{-3}$ mbar s/mL, and compliance, $C_{lung} = 60$ mL/mbar are used. These values are chosen based on the use cases in the ISO standard for pressure-controlled mandatory ventilation obtained from Table 201.104 in NEN-EN-ISO 80601-2-12:2011 (NEN, Delft, The Netherlands). The compliance value is a typical value for an adult. The resistance value is slightly higher than the airway resistance of a healthy human, because in between the sensors and the airway a bacterial filter is included for hygiene reasons. This filter increases the combined resistance significantly. Note that using other realistic parameters for the compliance and resistance results in similar conclusions, because the resulting overall shape is not affected significantly.

Using the estimated breathing effort and the different breathing effort models in (6) and (7), the parameters of the breathing effort models are determined such that the models resemble the estimated breathing effort accurately. The resulting breathing effort models are also depicted in the bottom plot of Fig. 4. This figure already shows that the flipped halfwave resembles the true effort more accurately.

Using the estimated lung parameters and effort models, the lung mechanics model in (5), and the measured airway pressure as an input, the resulting flow for both models is computed. This flow Q_{pat} is depicted in the middle plot of Fig. 4. The figure clearly shows that the simulated flow with the flipped halfwave resembles the measurements more accurately. From this result, it is concluded that the flipped halfwave resembles the true breathing effort significantly better.

Finally, errors for the patient flow $e_Q = Q_{pat,sim} - Q_{pat,exp}$ and the patient effort $e_{mus} = p_{mus,sim} - p_{mus,exp}$ are computed for both effort models. These errors are shown in Fig. 5. The figure clearly shows that both errors are significantly smaller when using the flipped halfwave. Also, the 2-norm of both patient flow errors are computed. The resulting 2-norm using the sinusoidal halfwave and flipped halfwave are 115.6 mbar and 54.3 mbar, respectively. Therefore, it is concluded that the flipped halfwave represents the true breathing effort significantly better.

The results of the considered test subject show that the proposed model can accurately describe human breathing. Furthermore, the resulting flow curve of the flipped halfwave model is much
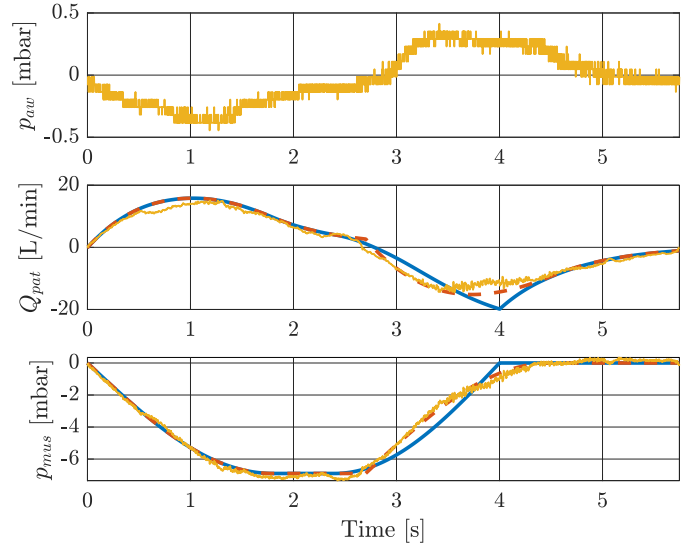

Fig. 4. Results of the experiments, showing the measurements of the test subject and its estimated effort (—) and the simulation results using the flipped halfwave (6) (- - -) and the sinusoidal halfwave (7) (—) effort models. From the figures, it is concluded that the overall shape of the flipped halfwave represents the measured breathing effort better during expiration.

smoother during the expiration phase. This smooth curve is a much more realistic representation of human expiration, which does not contain a sharp change in direction in the middle of the expiration. Therefore, we are confident that the proposed model can accurately describe human breathing. However, the flipped halfwave effort model should be analyzed in a larger group of test subjects to obtain more conclusive results.

Concluding, the experimental results clearly show that the flipped halfwave can accurately describe the breathing effort of a healthy test subject and gives a natural symmetrical flow pattern. Furthermore, it is shown that it resembles the effort significantly better than the commonly used sinusoidal halfwave. Therefore, we propose to consider the flipped halfwave breathing effort model when developing mechanical ventilators and analyzing the patient-ventilator interaction.

5. CONCLUSION

In this paper, a simple, intuitive model that accurately describes spontaneous breathing effort is presented. The presented model is significantly more accurate and results in more natural waveforms than the commonly used sinusoidal halfwave. The model presented in this paper can be used for research and development of mechanical ventilators, ventilation algorithms, and to improve understanding of a patient's breathing.

The next step is a further validation of the model on a large range of patients, both to investigate differences between patients, e.g., critically ill patients, as well as to further substantiate the accuracy of the flipped halfwave.

REFERENCES

Bates, J.H.T. (2009). *Lung Mechanics*. Cambridge University Press.

Blanch, L., Villagra, A., Sales, B., Montanya, J., Lucangelo, U., Luján, M., García-Esquirol, O., Chacón, E., Estruga,
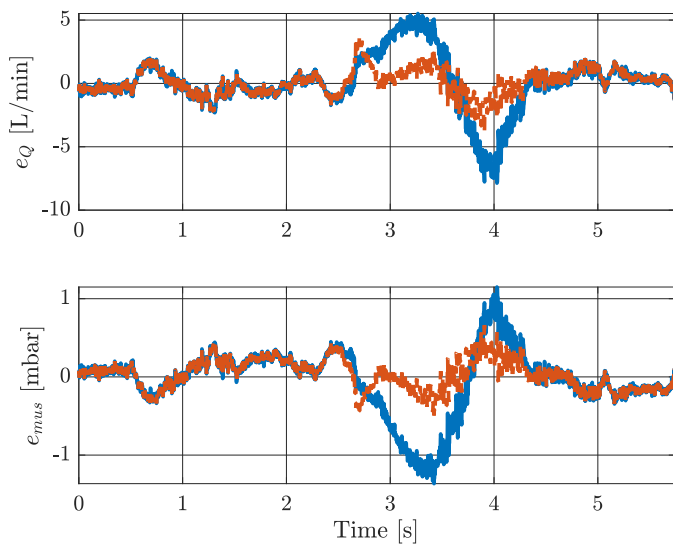
Fig. 5. Error plots of the experiments with the test subject, showing the flow error e_Q and the effort error e_{mus} for the flipped halfwave (6) (- - -) and the sinusoidal halfwave (7) (——) effort models. From the figures it is concluded that the flipped halfwave represents the measured breathing effort significantly better during expiration.

A., Oliva, J.C., Hernández-Abadia, A., Albaiceta, G.M., Fernández-Mondejar, E., Fernández, R., Lopez-Aguilar, J., Villar, J., Murias, G., and Kacmarek, R.M. (2015). Asynchronies during mechanical ventilation are associated with mortality. *Intensive Care Medicine*, 41(4), 633–641.

Borrello, M. (2001). Adaptive inverse model control of pressure based ventilation. In *Proceedings of the American Control Conference*, 1286–1291. Arlington, VA, USA.

Chiew, Y.S., Pretty, C., Docherty, P.D., Lambermont, B., Shaw, G.M., Desaive, T., and Chase, J.G. (2015). Time-varying respiratory system elastance: A physiological model for patients who are spontaneously breathing. *PLOS ONE*, 10(1), e0114847.

Epstein, S.K. (2011). How often does patient-ventilator asynchrony occur and what are the consequences? *Respiratory care*, 56, 25–38.

Fresnel, E., Muir, J.F., and Letellier, C. (2014). Realistic human muscle pressure for driving a mechanical lung. *EPJ Nonlinear Biomedical Physics*, 2(1).

Hunnekens, B., Kamps, S., and van de Wouw, N. (2020). Variable-gain control for respiratory systems. *Transactions on Control Systems Technology*, 28(1), 163–171.

Kim, K.T., Redmond, D.P., Morton, S.E., Howe, S.L., Chiew, Y.S., and Chase, J.G. (2017). Quantifying patient effort in spontaneously breathing patient using negative component of dynamic elastance. *IFAC-PapersOnLine*, 50(1), 5486–5491.

Mauri, T., Cambiaghi, B., Spinelli, E., Langer, T., and Grasselli, G. (2017). Spontaneous breathing: a double-edged sword to handle with care. *Annals of Translational Medicine*, 5(14), 292–292.

Navajas, D., Alcaraz, J., Peslin, R., Roca, J., and Farré, R. (2000). Evaluation of a method for assessing respiratory mechanics during noninvasive ventilation. *The European respiratory journal*, 16, 704–709.

Olivieri, C., Costa, R., Conti, G., and Navalesi, P. (2011). Bench studies evaluating devices for non-invasive ventilation: critical analysis and future perspectives. *Intensive Care Medicine*, 38(1), 160–167.

Reinders, J., Hunnekens, B., Heck, F., Oomen, T., and van de Wouw, N. (2021). Adaptive control for mechanical ventilation for improved pressure support. *IEEE Transactions on Control Systems Technology*, 29(1), 180–193.

Scheel, M., Schauer, T., Berndt, A., and Simanski, O. (2017). Model-based control approach for a CPAP-device considering patient's breathing effort. *IFAC-PapersOnLine*, 50(1), 9948–9953.

Thille, A.W., Rodriguez, P., Cabello, B., Lellouche, F., and Brochard, L. (2006). Patient-ventilator asynchrony during assisted mechanical ventilation. *Intensive Care Medicine*, 32(10), 1515–1522.

van Diepen, A., Bakkes, T.H.G.F., De Bie, A.J.R., Turco, S., Bouwman, R.A., Woerlee, P.H., and Mischi, M. (2021). A model-based approach to synthetic data set generation for patient-ventilator waveforms for machine learning and educational use.

van Drunen, E.J., Chiew, Y.S., Pretty, C., Shaw, G.M., Lambermont, B., Janssen, N., Chase, J.G., and Desaive, T. (2014). Visualisation of time-varying respiratory system elastance in experimental ARDS animal models. *BMC Pulmonary Medicine*, 14(1).

Vicario, F., Albanese, A., Karamolegkos, N., Wang, D., Seiver, A., and Chbat, N. (2015). Noninvasive estimation of respiratory mechanics in spontaneously breathing ventilated patients: A constrained optimization approach. *IEEE Transactions on Biomedical Engineering*, 1–1.

Warner, M.A. and Patel, B. (2013). Mechanical ventilation. In *Benumof and Hagberg's Airway Management*, 981–997. Elsevier.

Wells, C.R., Fitzpatrick, M.C., Sah, P., Shoukat, A., Pandey, A., El-Sayed, A.M., Singer, B.H., Moghadas, S.M., and Galvani, A.P. (2020). Projecting the demand for ventilators at the peak of the COVID-19 outbreak in the USA. *The Lancet Infectious Diseases*, 20(10), 1123–1125.

Yoshida, T., Uchiyama, A., Matsuura, N., Mashimo, T., and Fujino, Y. (2012). Spontaneous breathing during lung-protective ventilation in an experimental acute lung injury model. *Critical Care Medicine*, 40(5), 1578–1585.